Critical Field of Superconducting Aluminum as a Function of Pressure and Temperature above 0.3°K

E. P. HARRIS AND D. E. MAPOTHER
Materials Research Laboratory and Department of Physics, University of Illinois, Urbana, Illinois

(Received 10 July 1967)

Precise measurements have been made of the critical field of superconducting Al from 0.3°K to T_c, at pressures of 0, 3100, 5400, and 7200 psi. The data are extrapolated to $T=0$, yielding the values (at zero pressure) $H_0=104.93\pm0.2$ G, $\gamma=1.349\pm0.015$ mJ/mole °K² and $T_c=1.1793\pm0.003$°K. These values are used to calculate the superconducting electronic entropy and the deviation of the critical-field curve from a parabolic law. The results are compared with previous experimental work and with the Bardeen-Cooper-Schrieffer theory as extended by Clem to include effects of energy-gap anisotropy. The present work gives better agreement with previous calorimetric measurements of the thermodynamic properties of superconducting Al than do earlier published critical-field measurements. The shape of the critical-field curve shows no pressure dependence to within the experimental accuracy. Assuming that the shape of the critical-field curve is entirely independent of pressure, we find $d\ \ln H_0/d\ \ln V=19.2\pm0.4$, $d\ \ln T_c/d\ \ln V=16.4\pm1.1$, and $d\ \ln\gamma/d\ \ln V=6.65\pm3$. These results are in fair agreement with earlier $H_c(P, T)$ measurements of Al, although our result for $d\ \ln\gamma/d\ \ln V$ is about a factor of 3 larger than has been obtained from thermal expansion measurements.

I. INTRODUCTION

THIS paper reports new precise measurements of the critical field surface, $H_c(T, P)$, of pure Al. Data for pressures up to 490 atm and temperatures above 0.3°K have been obtained. The results are compared with earlier published measurements of the thermodynamic properties of superconducting Al.

II. EXPERIMENTAL METHOD

A. Apparatus

The apparatus used in the present work combines the features of a He^3 refrigerator and a high-pressure bomb using designs which have been separately described in some detail in previous reports.[1,2] As shown in Fig. 1 the same high-pressure bomb (I in Fig. 1) used in earlier work[2] is inverted and suspended from the bottom of the He^3 evaporation chamber (B). Thermal contact between the liquid He^3 and the specimen is encouraged by a heavy connecting member of tellurium copper (L). The internal pressure at the specimen is indicated by a capacitance dilatometer which measures the elastic extension of the bomb under pressure. Other details of the apparatus may be identified from the legend which accompanies Fig. 1.

B. Sample Preparation

The aluminum sample was a 1.25-in. length cut from 0.080-in. diam 99.9999% pure polycrystalline aluminum wire.[3] After cutting, the sample was cleaned and its ends rounded in a 10N solution of NaOH followed by a distilled water rinse.

The sample was annealed for 20 h at 633°C in a CO_2 atmosphere, after which it was cooled to room temperature at a rate of 27°C per hour. The CO_2 provided a reducing atmosphere which stabilized the oxidation of the sample surface.[4] The sample was then recleaned as before and placed in the cryostat.

C. Procedure

Our techniques for producing and measuring the hydrostatic pressure on the specimen have been described previously,[2] but will be briefly reviewed here. The bomb was thermally isolated from the He^4 bath and its temperature raised to about 1°K above the melting point of helium at the desired filling pressure. The bomb was then slowly filled with high pressure He^4 gas. The capacitance pressure gauge on the bomb was calibrated during filling by comparison with an external pressure gauge[5] in the gas system. After pressurizing the bomb, the inlet capillaries were frozen shut by putting them in thermal contact with the helium bath, and the bomb was cooled to the bath temperature over a period of several hours. The pressure drop during solidification was typically 30% of the filling pressure, consistent with the P-V-T measurements of Dugdale and Simon.[6] The final pressure of the three condensations performed were 3100, 5400, and 7200 psi. The condensation curve for the 5400 psi condensation is shown in Fig. 2.

The bomb capacitor (one plate of which was grounded) was measured by comparison with a precision variable capacitor,[7] using a capacitance bridge. The effects of variable lead capacitance were avoided through the use

* Work supported in part by the U.S. Army Research Office (Durham), and by the Advanced Research Projects Agency under Contract No. SD-131.

† Based upon the thesis submitted by E. P. H. in partial fulfillment of the requirements for the Ph.D. degree at the University of Illinois.

[1] D. K. Finnemore and D. E. Mapother, Phys. Rev. **140**, A507 (1965).

[2] M. Garfinkel and D. E. Mapother, Phys. Rev. **122**, 459 (1961).

[3] Cominco Products, Inc., Spokane, Wash.

[4] R. O. Simmons (private communication).

[5] Heise Bourdon Tube Company, Newton, Connecticut.

[6] J. S. Dugdale and F. E. Simon, Proc. Roy. Soc. (London) **A218**, 291 (1953).

[7] General Radio Model 1422-MD, General Radio Company, West Concord, Mass.

of a triaxial cable between the capacitance bridge and the bomb capacitor. An inner shield connected to the bridge output divided the lead capacitance (about 20 pF) into two parts. One part was across the bridge output and thus had no effect on the bridge balance. The other part was effectively in parallel with a 1000-pF capacitor in one arm of the bridge. Hence variations in bridge output due to variations in stray capacitance were reduced by a factor of about 1000 pF/C_{bomb}, or roughly by a factor of 20 from what would have been observed with a simple coaxial cable connection.

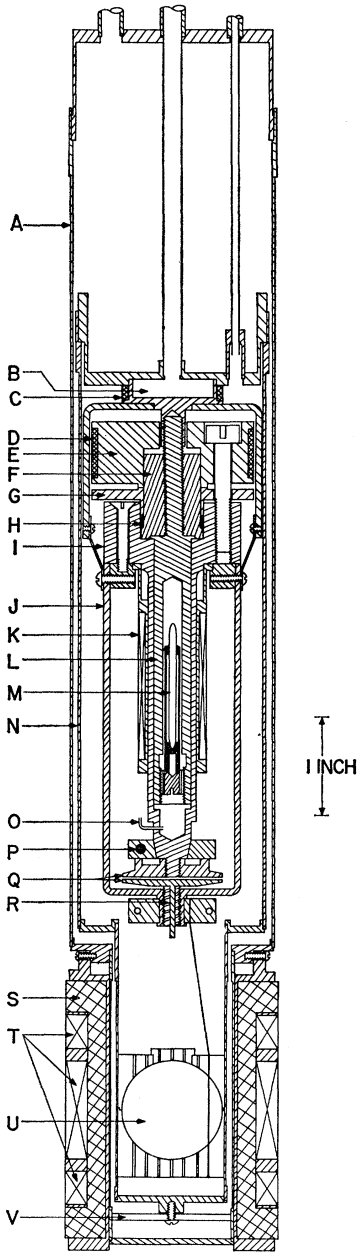

FIG. 1. Cross-section of cryostat. A—outer can; B—He^3 evaporation chamber; C—inner system heater; D—bucking coil; E—beryllium copper plug; F—flange; G—thrust washer; H—Teflon gasket; I—high pressure bomb; J—copper yoke; K—sample coil; L—thermal ground; M—sample; N—inner can; O—high-pressure capillaries; P—Speer carbon resistor; Q—capacitor plates; R—epibond insulator; S—salt pill primary coil; T—salt pill secondary coils; U—salt pill; V—nylon spacer.

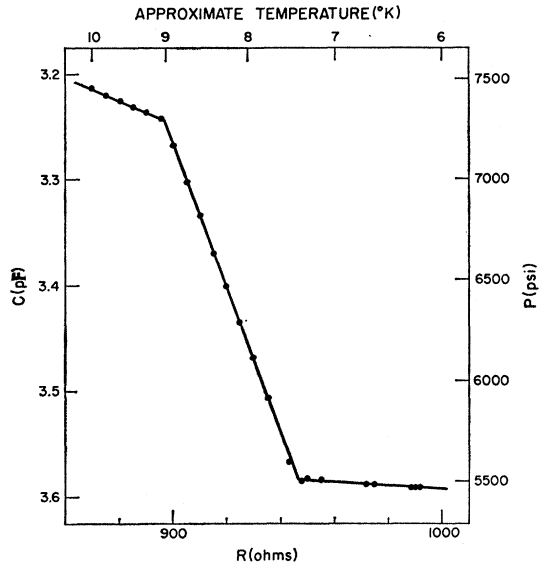

FIG. 2. Constant volume condensation of solid helium at 5400 psi.

Although the sensitivity of the capacitance dilatometer was about ±10 psi, long-term instability in the capacitance measuring system limited the accuracy of the pressure measurement to about ±200 psi. Hysteresis in the capacitance calibration of about 10% of the maximum pressure was observed for calibrations performed during the initial pressurization and depressurization of the bomb at low temperature. However, the calibrations performed thereafter were reproducible provided (a) the pressure was not increased above the maximum of the initial cycle, (b) the bomb was not warmed above roughly 25°K, and (c) the bomb was not subjected to sudden mechanical shock. The 5400 psi calibration may have been about 300 psi high due to incomplete cycling prior to calibration, but this would have a negligible effect on the results and will be ignored.

The ballistic induction technique used to measure H_c [8] and the procedure for controlling and measuring temperatures have been described previously.[1] A paramagnetic salt thermometer was provided for temperature calibration below 1°K.

III. ANALYSIS OF RESULTS

A. Details of Magnetic Transitions

A transition which is typical of all transitions taken below $t^2=0.6$ is shown in Fig. 3. The dashed line shows the transition shape corresponding to the demagnetiz-

[8] J. F. Cochran, D. E. Mapother, and R. E. Mould, Phys. Rev. 103, 1657 (1956).

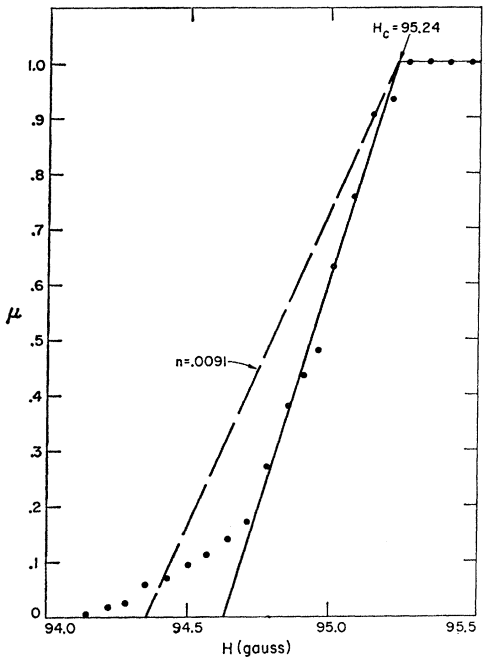

FIG. 3. Typical superconducting transition. This transition was measured at $T=0.3259$°K during the 3100 psi run.

ing factor calculated from the length to diameter ratio of the sample. All the transitions were somewhat narrower than would be predicted from the demagnetizing factor. This behavior has been observed before in aluminum by Cochran and Mapother,[9] and attributed to a large positive interphase surface-free energy.

Above $t^2=0.6$, superheating effects were observed. The transitions, although very sharp, were irregular in shape. However, the smoothness of the resulting critical field curves over the entire temperature range and the thermodynamic consistency of our data with calorimetric measurements of $\Delta C(T_c)$ (see Table IV) indicate that the critical-field values obtained in the high-temperature range must be very close (within about 0.1 G) to the equilibrium values.

Detailed measurements of supercooling were not made. During the first zero-pressure run, the supercooled transitions were about 16% lower than the corresponding superconducting-to-normal transitions. For all high-pressure runs, and for the second zero-pressure run, the supercooling was reduced to 5% of H_c. It should be noted that the second zero-pressure run was performed immediately after the 5400 and 7200 psi runs, without warming the sample above 15°K. The first zero-pressure run was made immediately after cooling down from room temperature. Although there was no broadening of the superconducting-to-normal transitions, it seems clear that the pressure induced some permanent change in the sample which reduced the supercooling. However, critical-field curves obtained from the two zero-pressure runs (see Fig. 7) are in excellent agreement, indicating that any change in the sample did not affect the critical field to within our experimental uncertainty.

The critical-field data are listed in Table I. The zero-pressure listing includes the data from both zero-pressure runs.

B. Analysis of Critical Field Curves

Thermodynamic analysis of critical-field data proceeds from the equation[10]

$$\Delta S=S_n-S_s=-(VH_c/4\pi)(\partial H_c/\partial T)_P, \quad (1)$$

where S_n and S_s are the normal and superconducting molar entropies and V is the molar volume. Making the usual assumptions that the lattice entropy is unchanged in the superconducting transition, and that the normal electronic entropy S_{en} is given by γT,[1] the above equation can be integrated over the temperature range 0 to T to give

$$H_c^2=H_0^2[1-(4\pi\gamma T_c^2/VH_0^2)[t^2-2g(t)]], \quad (2)$$

where $t=T/T_c$ and

$$g(t)=\int_0^t\left(\frac{S_{es}}{\gamma T_c}\right)dt=\int_0^t\left\{\int_0^t\left(\frac{C_{es}}{\gamma T_c}\right)\frac{dt}{t}\right\}dt; \quad (3)$$

S_{es} and C_{es} are the electronic contributions to S_s and C_s. The BCS theory[11] predicts (and it is experimentally confirmed[1]) that $g(t)$ approaches zero much faster than t^2. For $t\lesssim 0.25$, $2g(t)$ is negligibly small compared to t^2. Hence, in the low-temperature limit,

$$H_c^2=H_0^2-(4\pi\gamma/V)T^2. \quad (4)$$

Provided experimental data exist in the region below $t=0.25$, Eq. (4) can be used to find H_0 and γ by fitting the low-temperature data to a straight line in a plot of H_c^2 versus T^2.[1,12] Once H_0 and γ are determined, S_{es} may be determined from the data by using Eq. (1). If insufficient low-temperature data are available, then one must have knowledge of the behavior of $g(t)$ in order to obtain γ and H_0. This, of course, is equivalent to knowing the form for S_{es}, but it turns out that neither γ nor H_0 are very sensitive to the details of $g(t)$ in the region $0.25\lesssim t\lesssim 0.5$, where $g(t)$ is small but not negligible. Thus the final form of S_{es} calculated from the data over the entire temperature range is not sensitive to its assumed behavior in the region where it is small.

For aluminum, $T_c\cong 1.18$°K; hence $t=0.25$ corresponds to about $T=0.295$°K, which is about the lowest temperature attainable with the He^3 refrigerator here. Thus, to find H_0 and γ, the critical-field data must be fit to Eq. (2), using an estimated form for

[9] J. F. Cochran and D. E. Mapother, Phys. Rev. 111, 132 (1958).

[10] D. Shoenberg, *Superconductivity* (Cambridge University Press, Cambridge, England, 1952), 2nd ed.

[11] J. Bardeen, L. N. Cooper, and J. R. Schrieffer, Phys. Rev. 108, 1175 (1957).

[12] C. A. Swenson, IBM J. Res. Develop. 6, 82 (1962).

TABLE I. Critical-field data for aluminum.

H_c (G)	T(°K)	H_c (G)	T(°K)	H_c (G)	T(°K)	H_c (G)	T(°K)
$P=0$ psi		28.52	0.9845	71.20	0.6248	60.65	0.7176
96.95	0.3082	28.17	0.9852	66.79	0.6671	53.33	0.7811
96.58	0.3142	25.48	1.0062	61.18	0.7181	43.52	0.8603
96.25	0.3207	23.50	1.0183	53.85	0.7814	34.93	0.9264
95.80	0.3276	22.23	1.0291	44.08	0.8602	27.08	0.9854
95.28	0.3372	18.78	1.0533	40.00	0.8916	22.49	1.0183
95.85	0.3430	18.49	1.0543	35.46	0.9262	17.27	1.0543
94.66	0.3477	16.60	1.0685	30.04	0.9659	13.51	1.0801
94.00	0.3593	14.74	1.0801	27.69	0.9848	9.45	1.1074
93.49	0.3654	14.32	1.0843	24.62	1.0065	5.09	1.1366
93.11	0.3724	11.89	1.1006	21.34	1.0295	1.36	1.1613
92.17	0.3870	10.69	1.1074	17.83	1.0537		
92.21	0.3871	9.36	1.1176	15.65	1.0687	$P=7200$ psi	
91.09	0.4038	6.66	1.1352	13.53	1.0847		
91.01	0.4038	6.48	1.1366	10.92	1.1011	95.06	0.3166
89.69	0.4226	3.95	1.1535	8.46	1.1181	94.46	0.3257
88.87	0.4339	1.76	1.1676	5.73	1.1357	93.92	0.3358
88.06	0.4445	1.01	1.1726	2.91	1.1540	93.26	0.3471
85.95	0.4711	$P=3100$ psi		1.01	1.1666	92.14	0.3654
85.88	0.4717			$P=5400$ psi		90.69	0.3870
83.43	0.5028	96.37	0.3056			89.54	0.4037
83.29	0.5028	96.07	0.3120	96.81	0.2905	87.35	0.4337
80.13	0.5408	95.67	0.3188	96.30	0.3000	84.41	0.4717
79.86	0.5415	95.24	0.3259	95.87	0.3087	8.185	0.5025
75.41	0.5890	94.76	0.3354	95.33	0.3181	78.41	0.5417
75.37	0.5910	94.12	0.3459	94.87	0.3268	73.76	0.5901
71.92	0.6256	93.40	0.3577	94.30	0.3365	65.79	0.6671
67.46	0.6669	92.59	0.3707	93.69	0.3471	60.19	0.7180
67.42	0.6672	91.63	0.3855	92.52	0.3653	52.90	0.7810
61.88	0.7175	90.50	0.4022	91.16	0.3869	43.01	0.8603
61.95	0.7179	89.12	0.4214	89.99	0.4036	34.40	0.9264
54.58	0.7810	87.50	0.4438	87.82	0.4334	26.30	0.9852
44.85	0.8600	86.73	0.4537	84.94	0.4715	21.78	1.0183
44.76	0.8603	85.48	0.4700	82.19	0.5026	16.74	1.0543
40.87	0.8914	82.81	0.5014	78.88	0.5415	12.94	1.0801
36.37	0.9259	79.36	0.5409	74.12	0.5903	8.82	1.1074
36.09	0.9264	74.72	0.5893	66.20	0.6671	4.51	1.1366
31.09	0.9656					1.66	1.1550

$g(t)$. Phillips[13] found that in the range $0.3<t<0.5$, the superconducting electronic specific heat can be adequately represented by

$$(C_{es}/\gamma T_c)=7.1\exp(-1.34/t). \quad (5)$$

Phillips' measurements in this temperature range appear to be the best available calorimetric data on Al at present. Using Eq. (5) to calculate (3), we have fit the experimental data to Eq. (2) for $t<0.5$, thus yielding values for H_0 and γ at each pressure. We have assumed that $g(t)$ is independent of pressure.

Values of T_c and $(\partial H_c/\partial T)_P$ at T_c were obtained by extrapolating the data for $t^2\geq 0.9$ to $H_c=0$ using a straight-line fit of H_c versus T^2 which, as shown in Fig. 11, represents our data within the limits of experimental accuracy.

The results calculated are presented in Table II. The error limits in Table II include the effects of absolute error estimates on the low- and high-temperature extrapolations of the data and the uncertainty in the results due to scatter in the measurements. The error limits do not include the effects of possible errors in Phillips' specific-heat results.

To display the data on a more sensitive scale we may define the fiducial function[1]

$$H_c^2=H_0^2-(4\pi\gamma/V)T^2. \quad (6)$$

TABLE II. Parameters deduced from critical-field curves.[a]

Pressure (psi)	H_0 (G)	γ (mJ/mole °K²)	T_c(°K)	$2\pi\gamma T_c^2/VH_0^2$	$(\partial H_c/\partial T)_P$ at T_c (G/°K)	$\Delta C(T_c)$ (mJ/mole °K)
0	104.93±0.2	1.349±0.015	1.1793±0.003	1.0846	−155±2	2.22±0.06
3100	104.25±0.2	1.337±0.015	1.1732±0.003	1.0780	−155±2	2.21±0.06
5400	103.95±0.2	1.341±0.015	1.1701±0.003	1.0827	−155±2	2.21±0.06
7200	103.58±0.2	1.343±0.015	1.1659±0.003	1.0842	−155±2	2.20±0.06

[a] The molar volume of aluminum was taken to be 9.87 cc/mole (Ref. 36) at zero pressure. At higher pressures this value was corrected, using for the compressibility $k_n=1.34\times10^{-6}$ atm^{-1}, (Ref. 17).

[13] N. E. Phillips, Phys. Rev. 114, 676 (1959).

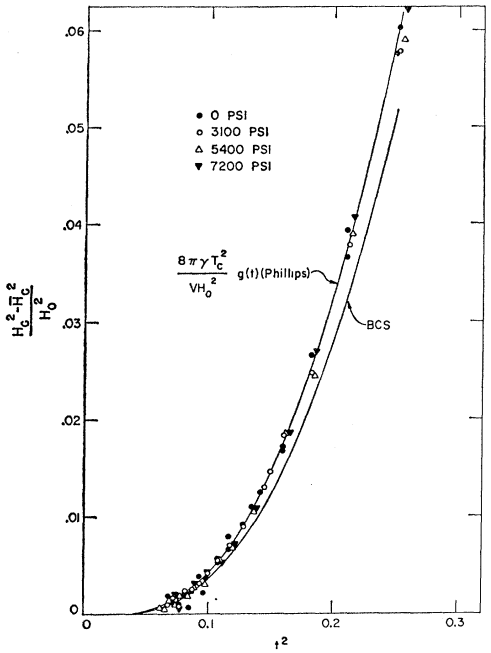

FIG. 4. Deviation of the critical field from $H_c^2=H_0^2-(4\pi\gamma/V)T^2$. Values for H_0, γ, and T_c used are those given in Table II. Also plotted are the theoretical BCS curve and the curve calculated from the specific heat results of Ref. 13.

In Fig. 4, we plot the deviation of the observed H_c^2 from this fiducial function in units of H_0^2, using values of H_0, T_c, and γ from Table II. From Eq. (2), this deviation is given by

$$(H_c^2-H_c^2)/H_0^2=(8\pi\gamma T_c^2/VH_0^2)g(t). \qquad (7)$$

This plot shows the quality of the fit to $g(t)$ as calculated from Phillips' measurements of the low-temperature superconducting electronic specific heat. Also shown is the curve calculated from the BCS theory. If the BCS result for $g(t)$, which lies about 15% lower than the Phillips result for $0.1<t^2<0.25$, had been used to calculate H_0 and γ, the resulting value of H_0 would have been about 0.1 G lower than that given in Table II, and γ would have been about 1% lower.

The critical field curves are presented in Fig. 5, in terms of their deviation from a fiducial parabola

$$D(t)=H_c/H_0-(1-T^2/T_c^2), \qquad (8)$$

using the value of H_0 and T_c from Table II. There is no significant pressure dependence of the shape of the deviation function. If the BCS $g(t)$ had been used to find H_0, thus changing H_0 by $0.001H_0$, the deviation functions $[D(t)]$ would have been shifted up by $0.001H_c/H_0$, which is 0.0005 at $t^2=0.5$. They still would be in much better agreement with Phillips' results than with the deviation function calculated from BCS.

ΔS was calculated from Eq. (1), where the derivative $(\partial H_c/\partial T)_p$ was evaluated at each point by fitting a few points in the neighborhood of a given point to $H_c=a+bT^2$. In most cases, three points on either side of the point in question were used. In Fig. 6, $(S_{es}/\gamma T_c)$ is displayed for all the data. The $(S_{es}/\gamma T_c)$ curves are nearly identical for all pressures, and lie slightly above the BCS curve.

C. Effect of Pressure on Critical-Field Curves

In the previous section it was shown that γ could be extracted from measurements of $H_c(T)$. Clearly, if critical-field curves are measured at a series of pressures, γ can be determined for each pressure, and, in principle at least, the pressure dependence of γ can be studied. This analysis was in fact carried out for the data reported here, and the resulting γ values are listed in Table II. Unfortunately, the change in γ produced by the available pressures is quite small (on the order of 1%), and is obscured in the scatter. This scatter is due primarily to the uncertainties in extrapolating the low-temperature data to $T=0$. Some basis is necessary for finding the change in γ with pressure which will remove some of the extrapolation uncertainty.

A plausible approach to this question is suggested by the data of Fig. 5 which strongly suggest that the analytic form of the critical-field curve is invariant under pressure. This is certainly true within the experimental uncertainty of the present measurements, and, to our knowledge, all available measurements of

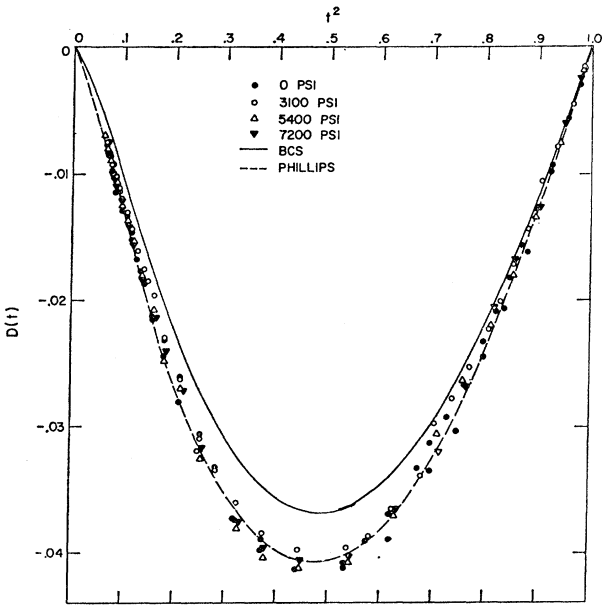

FIG. 5. Experimental results for the deviation function $D(t)=H_c/H_0-1+T^2/T_c^2$ plotted versus the square of the reduced temperature, using H_0 and T_c values from Table II. The solid curve represents the theoretical BCS result. The dashed curve represents specific-heat results of Ref. 13. Above $t^2=0.25$ the dashed curve was scaled from Fig. 10 of Ref. 13. Below $t^2=0.25$ it was calculated from Eq. (5).

$H_c(P, T)$ except for those on Sn [14] give results consistent with this conclusion.

A formal statement of this assumed invariance has become known in past literature[15,16] and recent research[17,18] as the "similarity principle" and may be written as

$$H_c(P, t) = H_0(P) f(t), \tag{9}$$

where $f(t)$ is a function independent of pressure. From Eq. (2) we see that the similarity principle implies that the characteristic superconducting constant

$$K = 2\pi\gamma T_c^2 / V H_0^2 \tag{10}$$

is unchanged by the pressure. The present measurements indicate that K is constant to $\pm 0.35\%$ and,

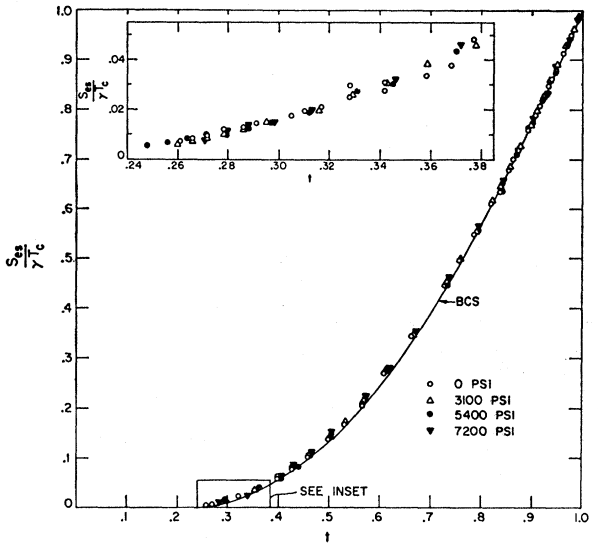

FIG. 6. Superconducting electronic entropy calculated from the experimental data (see text), using values of γ and T_c from Table II. Each point plotted below $t=0.38$ represents the average of 4 entropy points calculated from the data. In the inset, the portion of the graph below $t=0.38$ is enlarged, showing all the entropy points. Also plotted is the theoretical BCS curve.

while further and more sensitive tests may be desirable, we base the subsequent analysis on the assumptions that the shape of the critical-field curve is independent of pressure and that K is, in fact, constant. Differentiating (10) we obtain

$$\frac{d\ln K}{d\ln V} = 0 = \frac{d\ln\gamma}{d\ln V} - 1 + 2\left(\frac{d\ln T_c}{d\ln V}\right) - 2\left(\frac{d\ln H_0}{d\ln V}\right)$$

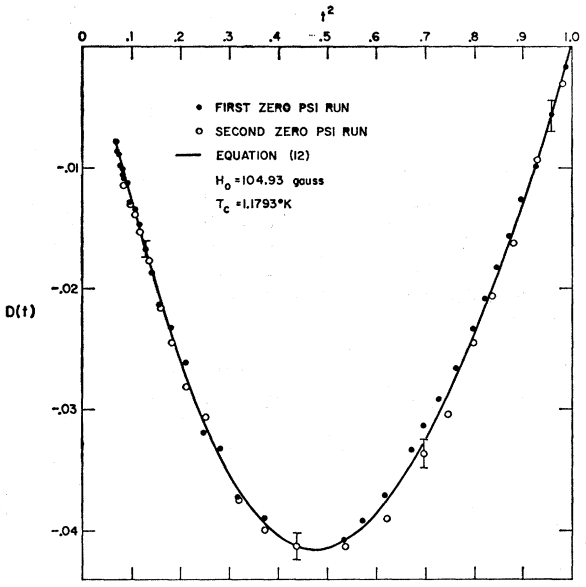

FIG. 7. Zero-pressure results for the deviation function. The error bars are estimates of the limit of relative error. The solid curve is a polynomial function [Eq. (12)] which is a best least-squares fit to the data.

or

$$\frac{d\ln\gamma}{d\ln V} = 1 - 2\left[\frac{d\ln T_c}{d\ln V} - \frac{d\ln H_0}{d\ln V}\right]. \tag{11}$$

Thus, under the assumption of similarity, the volume dependence of γ may be calculated from the pressure dependence of the intercepts, T_c and H_0.

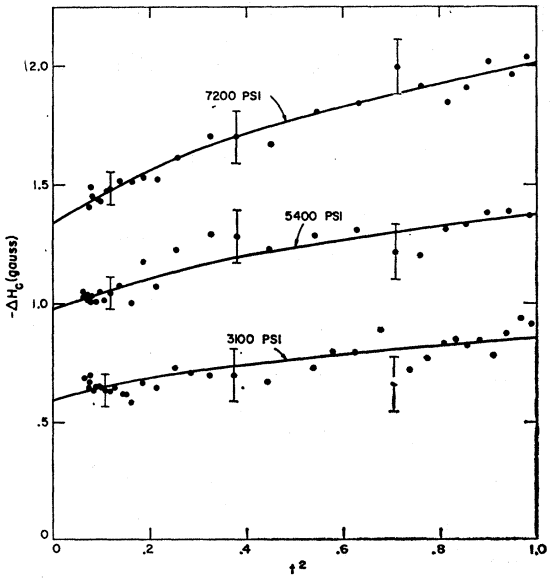

FIG. 8. The pressure shift of the critical field defined by $\Delta H_c(P, T) = H_c(P, T) - H_c(O, T)$, where $H_c(O, T)$ is given by Eq. (12), is plotted versus the square of the reduced temperature. The values of T_c at each pressure are taken from Table II. The error bars are estimates of the limit of relative error. The solid curves represent the best least-squares fit to the data assuming similarity.

[14] J. E. Schirber and C. A. Swenson, Phys. Rev. **127**, 72 (1962).
[15] J. L. Olsen and H. Rohrer, Helv. Phys. Acta **33**, 872 (1960).
[16] C. A. Swenson, in *Solid State Physics*, edited by F. Seitz and D. Turnbull (Academic Press Inc., New York, 1960), Vol. II, p. 41.
[17] N. B. Brandt and N. I. Ginzburg, Usp. Fiz. Nauk **85**, 485 (1965) [English transl.: Soviet Phys.—Uspekhi **8**, 202 (1965)].
[18] M. Levy and J. L. Olsen, in *Physics of High Pressure*, edited by A. van Itterbeek (North-Holland Publishing Company, Amsterdam, 1965).

TABLE III. Pressure shift of the endpoints of the critical-field curve.

Pressure (psi)	Results from similarity analysis[a] ΔH_0 (G)	$\Delta H_c(P, T_c)$ (G)	ΔT_c (°K)	Results from direct analysis of individual critical-field curves[b] ΔH_0 (G)	$\Delta H_c(P, T_c)$ (G)	ΔT_c (°K)
3100	−0.589±0.016	−0.850±0.043	−0.0055	−0.68	−0.94	−0.0061
5400	−0.979±0.018	−1.380±0.052	−0.0089	−0.98	−1.43	−0.0092
7200	−1.335±0.018	−2.007±0.047	−0.0130	−1.35	−2.08	−0.0134

[a] See text; Eq. (16) was used to find ΔT_c, with $(\partial H_c/\partial T)_g = -155$ G/°K at T_c.

[b] Calculated from Table I, using (16) to find ΔT_c, with $(\partial H_c/\partial T_c) = -155$ G/°K at T_c.

Two methods are available to us for calculating the pressure dependence of T_c and H_0. We could simply use the values of $T_c(P)$ and $H_0(P)$ listed in Table II, or, on the basis of (9) we could find the values of $\Delta T_c(P) = T_c(P) - T_c(0)$ and $\Delta H_0(P) = H_0(P) - H_0(0)$ which minimize the pressure dependence of the shape of the critical-field curve. The second method gives minimum scatter, since $\Delta H_0(P)$ and $\Delta T_c(P)$ are obtained by assuming a temperature dependence for the entire critical-field curve $H_c(P, T)$ rather than by extrapolating only the data close to $T = T_c$ and $T = 0$. It is important for this analysis that we have an accurate measurement of $f(t)$ over a wide temperature range. Most prior investigations of the pressure effect (particularly in Al) have based their analysis on the assumption of the parabolic law, $f(t) = 1 - t^2$.[19] The present analysis treats $T_c(0)$ and $H_0(0)$ as independent parameters determined separately from observations near 0°K and T_c, and treats $f(t)$ as a smooth curve determined from measurements of $H_c(T)$ at zero pressure over a wide temperature range.

The zero-pressure data and a curve fit to the data in least-squares fashion are displayed in Fig. 7. The function used is

$$H_c = \sum_{i=0}^{6} a_i (t^2)^i, \qquad (12)$$

where

$$a_0 = 105.19795, \quad a_4 = -63.221601,$$
$$a_1 = -121.47833, \quad a_5 = 25.785877,$$
$$a_2 = -1.4105433, \quad a_6 = -2.5004711,$$
$$a_3 = -57.608482, \quad T_c = 1.1793\text{°K}$$

for $0.06 \leq t^2 \leq 1.0$.

In Fig. 8, the difference

$$\Delta H_c(S) = H_c(P, T) - H_c(0, T),$$

where $H_c(0, T)$ is calculated from (12), is plotted versus $[(T/T_c(P)]^2$. Using the similarity principle, it is easily shown by differentiating (9) that

$$\Delta H_c(P) = \Delta H_0(P) \left[1 + \left(2 \frac{d \ln T_c/dP}{d \ln H_0/dP} - 1 \right) t^2 + D(t) - 2t^2 \frac{\partial D}{\partial t^2} \frac{d \ln T_c/dP}{d \ln H_0/dP} \right], \qquad (13)$$

where $D(t)$ has been previously defined. The solid curves in Fig. 8 represent the best least-squares fit of this equation to the $\Delta H_c(P)$ data. Note that the fit must be made in a self-consistent way, since $[(d \ln T_c/dP)/(d \ln H_0/dP)]$ is not known and is pro-

TABLE IV. Compilation of zero-pressure magnetic and calorimetric results for aluminum.

Reference	H_0 (G)	T_c (°K)	γ (mJ/mole °K²)	$2\pi\gamma T_c^2/VH_0^2$	$(\partial H_c/\partial T)_P$ at T_c (G/°K)	Cal. $\Delta C(T_c)$ (mJ/mole °K)	Mag. $\Delta C(T_c)$ (mJ/mole °K)
Cochran and Mapother[a]	99±1	1.196±0.005			−165.5		2.57
Caplan and Chanin[b]	104.8±0.6	1.175±0.001	1.23–1.30	1.061	−158±4		2.31±0.12
Rorer *et al.*[c]		1.173–1.188			−153	2.21	2.19±0.03
Hopkins and Mapother[d]		1.1797±0.0003			−152	2.21	2.14
Phillips[e]	103.0	1.163	1.35±0.01	1.088	−152	2.10	
This work	104.93±0.2	1.1793±0.003	1.349±0.015	1.085	−155±2		2.22±0.06

[a] See Ref. 9. The results obtained by Cochran and Mapother are superceded by the present work.

[b] See Ref. 24.

[c] See Ref. 21.

[d] See Ref. 22.

[e] See Refs. 13 and 23.

[19] See, for instance, Ref. 18.

portional to $\Delta H_c(P, T_c)/H_0(P)$. The procedure used to find the best fit was as follows.

We define a function $u(t^2)$ given by

$$u(t^2)=1+\left\{2\left(\frac{d\ln T_c/dP}{d\ln H_0/dP}\right)\left[1-\left(\frac{\partial D}{\partial t^2}\right)_{T_c}\right]-1\right\}t^2. \quad (14)$$

The function $u(t^2)$ is a straight line passing through the endpoints of (13). We then define a parameter t^* such that

$$u(t^{*2})=1+\left[2\frac{d\ln T_c/dP}{d\ln H_0/dP}-1\right]t^2 + D(t)-2t^2\frac{\partial D}{\partial t^2}\frac{d\ln T_c/dP}{d\ln H_0/dP}. \quad (15)$$

Thus the analytic form for $\Delta H_c(P)$ given by (13) is a straight line when plotted versus t^{*2}, although it is curved when plotted versus t^2. The dependence of t^{*2} on t^2 depends on the shape of $D(t)$ and the value of $[(d\ln T_c/dP)/(d\ln H_0/dP)]$. The functional form of $D(t)$ is determined from (12). We then evaluate t^{*2} versus t^2 by estimating $[(d\ln T_c/dP)/(d\ln H_0/dP)]$ on the basis of a straight-line fit of the $\Delta H_c(P)$ data versus t^2. Fitting the $\Delta H_c(P)$ data versus t^{*2} to a straight line then yields a new set of endpoints $[\Delta H_c(P, T_c)$ and $\Delta H_0(P)]$ which are used to make a better estimate of $[(d\ln T_c/dP)/(d\ln H_0/dP)]$. This value is then used to recalculate t^{*2} versus t^2, and a new fit of $\Delta H_c(P)$ versus t^{*2} is made. Carrying this procedure beyond two iterations produces negligible changes in the endpoints.

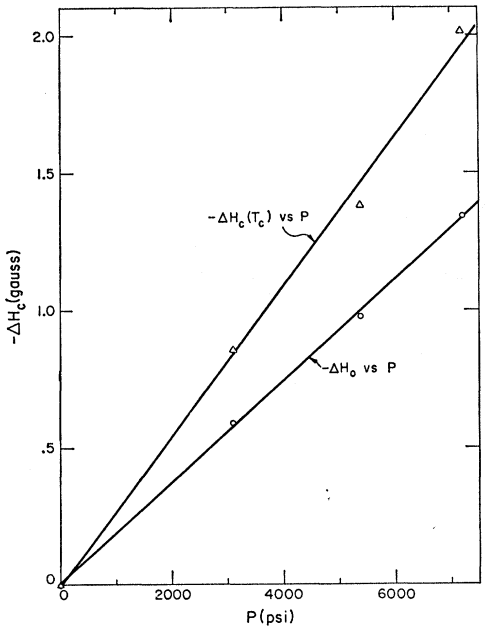

FIG. 9. The pressure shifts at $T=0$ and $T=T_c(P)$ are plotted versus pressure. These pressure shifts are the endpoints of the solid curves in Fig. 8, and are tabulated in Table III. The fact that each $\Delta H_c(T_c)$ is evaluated at $T_c(P)$ instead of $T_c(O)$, for instance, makes negligible difference (less than 0.01 G) in each case. The solid lines represent the best least-squares fit straight lines.

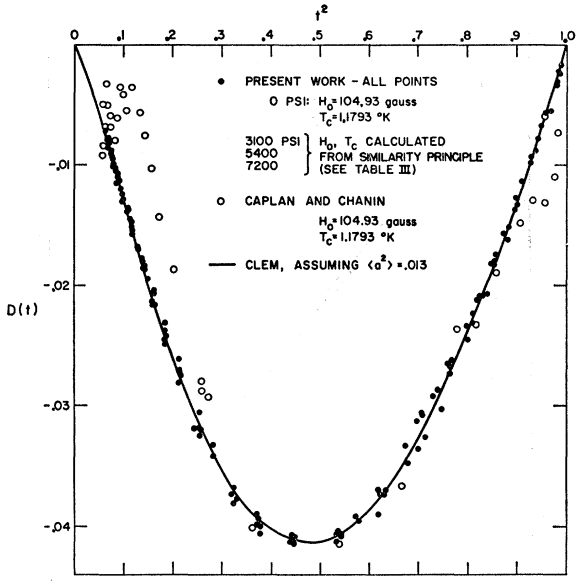

FIG. 10. The deviation function $D(t)=H_c/H_0-1+T^2/T_c^2$ is plotted using values of H_0 and T_c at zero pressure from Table II. Values for H_0 and T_c at nonzero pressure were calculated using the zero-pressure values in Table II and the pressure shifts in Table III calculated from the similarity principle. Points at all pressures are plotted with the same symbol. Also plotted are the data of Caplan and Chanin (Ref. 23) using our zero pressure H_0 and T_c. The theoretical calculation of Clem (Ref. 25) assuming $\langle a^2\rangle=0.013$ is represented by the solid curve.

In Table III the values of $\Delta H_c(P)$ at the endpoints of the solid curves in Fig. 8 are listed. The uncertainties represent standard deviations computed from least-squares analysis formulas.[20] Note that near T_c, $\Delta H_c(P, T)$ and ΔT_c are related by

$$-\Delta H_c(P, T_c)=\Delta T_c(P)[\partial H_c(T_c)/\partial T]_P. \quad (16)$$

Also, tabulated in Table III are values taken from Table II, which are subject to the extrapolation uncertainties mentioned earlier in this section. The agreement between the two sets of numbers is good.

The endpoints calculated from the similarity principle are plotted in Fig. 9, from which values for $(dH_0/dP$ and $(\partial H_c/\partial P)_{T=T_c}$ have been extracted by fitting the points to straight lines in least-squares fashion. We find

$$(dH_0/dP)=-(2.70\pm0.06)\times10^{-3}\ \text{G/atm}, \quad (17)$$

$$(\partial H_c/\partial P)_{T=T_c}=-(4.01\pm0.2)\times10^{-3}\ \text{G/atm}. \quad (18)$$

Again, the error bars denote standard deviations computed from least-squares analysis formulas.[20]

Then, using the value, $k_n=1.34\times10^{-6}\ \text{atm}^{-1}$, for the isothermal compressibility.[17] we find for the volume

[20] Yardley Beers, *Introduction to the Theory of Error* (Addison-Wesley, Publishing Co., Reading, Mass., 1958), Chap VI, Sec. B.

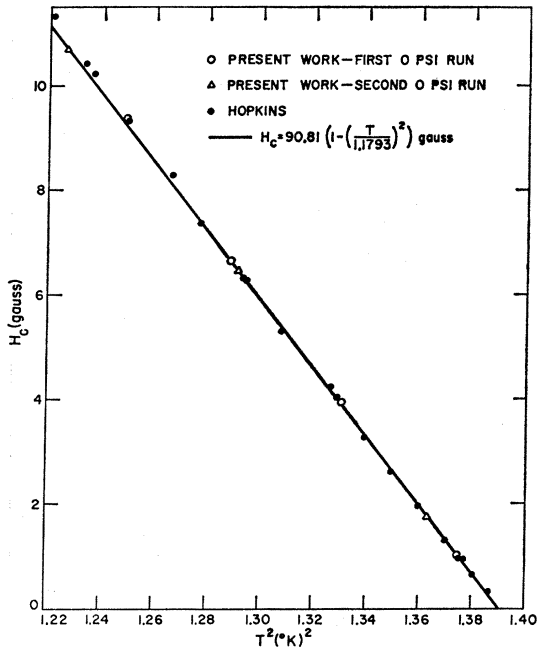

FIG. 11. Our zero-pressure data near T_c and the data of Hopkins (Ref. 22) are plotted versus T^2. The solid line has a slope of -154 G/°K at $T_c=1.1793$°K.

derivatives of T_c and H_0

$$\frac{d\ln T_c}{d\ln V}=\frac{(\partial H_c/\partial P)_{T=T_c}}{k_n T_c(\partial H_c/\partial T)_{P,T=T_c}}=16.4\pm1.1, \quad (19)$$

$$d\ln H_0/d\ln V=19.2\pm0.4. \quad (20)$$

We may now use (11) to calculate the value

$$d\ln\gamma/d\ln V=6.65\pm3. \quad (21)$$

IV. COMPARISON WITH OTHER RESULTS

The agreement of our zero-pressure measurements with previous results can be seen by comparing our parameters listed in Table IV with the calorimetric data of Phillips,[13] Rorer *et al.*,[21] and Hopkins[22] listed there also. The present magnetic measurements show better thermodynamic consistency with calorimetric results than with earlier H_c data. The degree of consistency can be seen by observing (Fig. 5) that our deviation function, $D(t)$, is practically identical to that calculated from Phillips' data. The only discrepancies between our data and those of Phillips are in the values of H_0 and T_c, where the results differ by about 1 to 2%.[23]

In Fig. 11, our high-temperature zero-pressure data are plotted on the same graph with the data of Hopkins, which were taken on a large spherical single crystal. The agreement with Hopkins' data is excellent.

Although our values of H_0 and T_c agree with those of Caplan and Chanin,[24] our results for $D(t)$ differ markedly from theirs at low temperatures. The two

TABLE V. Comparison of theoretical values of $2\Delta(0)/kT_c$ with thermodynamic data.

	Theory	H_c data
BCS calculations	3.53[a]	3.48±0.02[b]
Clem calculations	3.46[c]	3.43±0.02[d]

[a] From Eq. (23).
[b] From Eq. (22).
[c] From Eq. (25), with $\langle a^2\rangle=0.013$.
[d] From Eq. (24), with $\langle a^2\rangle=0.013$.

[21] D. C. Rorer, H. Meyer, and R. C. Richardson, Z. Naturforsch. **18a**, 130 (1963).
[22] D. C. Hopkins, thesis, University of Illinois, 1962 (unpublished).

TABLE VI. Compilation of experimental values of a $2\Delta(0)/kT_c$ for Al.

1. Measurements on bulk specimens

Reference	$2\Delta(0)/kT_c$	Method
Biondi and Garfunkel[a]	3.25±0.1	Surface resistance (polycrystal)
Biondi, Garfunkel, and Thompson[b]	3.04; 3.50±0.05	Surface resistance (single crystal)
Masuda and Redfield[c]	3.2	Nuclear spin relaxation time
David and Poulis[d]	3.7±0.3	Ultrasonic attenuation

2. Measurements on thin films by tunneling

Reference	$2\Delta(0)/kT_c$
Shapiro *et al.*[e]	2.5±0.3
Douglass and Meservey[f]	2.75–3.4
Zavaritskii[g]	3.37±0.1
Giaever and Megerle[h]	4.2±0.6

[a] M. Biondi and M. Garfunkel, Phys. Rev. **116**, 853 (1959).
[b] See Ref. 27.
[c] See Ref. 26.
[d] R. David and N. Poulis, in *Proceedings of the Eighth International Conference on Low-Temperature Physics, London, 1962*, edited by R. O. Davies (Butterworths Scientific Publications Ltd., London, 1963), p. 193.
[e] S. Shapiro, P. Smith, J. Nicol, J. Miles, and P. Strong, IBM J. Res. Develop. **6**, 34 (1962).
[f] D. Douglass, Jr. and R. Meservey, in *Proceedings of the Eighth International Conference on Low-Temperature Physics, London, 1962*, edited by R. O. Davies (Butterworths Scientific Publications Ltd., London, 1963), p. 180; Phys. Rev. **135**, A19 (1964).
[g] N. V. Zavaritskii, Zh. Eksperim. i Teor. Fiz. **41**, 657 (1961) [English transl.: Soviet Phys.—JETP **14**, 470 (1962)].
[h] I. Giaever and K. Megerle, Phys. Rev. **122**, 1101 (1961).

[23] W. H. Lien and N. E. Phillips have made recent measurements of C_n and C_s for Al, from which they calculate $H_0=105.0$ G, $T_c=(1.172\pm0.002)$°K, $\gamma=1.37$ mJ/mole °K², and $D_0=$maximum value of $D(t)=-0.0411$. Aside from their T_c value, their results are in excellent agreement with ours. Dr. Phillips has since reported to us that he has made an accurate measurement of T_c for Al, the result of which is in much better agreement with our value. We are indebted to Dr. Lien and Dr. Phillips for communicating their results to us prior to publication.
[24] S. Caplan and G. Chanin, Phys. Rev. **138**, A1428 (1965).

TABLE VII. Compilation of pressure effect and thermal expansion results for aluminum.

Reference	(dH_0/dP) (G/atm)	$(\partial H_c/\partial P)\,T=T_c$ (G/atm)	$\beta_{en}{}^{a}/T$ (°K^{-2})	$\beta_{gn}{}^{a}/T^3$ (°K^{-4})	$d\ln\gamma/d\ln V$
Olsen[b]	-11.5×10^{-3}	-4.0×10^{-3}			130±60
Gross and Olsen[c]	$(-3.1\pm0.2)\times10^{-3}$	$(-4.8\pm0.4)\times10^{-3}$			5.65±3
White[d]			$(27.3\pm1)\times10^{-10}$	$(7.8\pm0.6)\times10^{-11}$	1.51±0.05
Andres[e]			$(33\pm9)\times10^{-10}$	$(7.2\pm1.5)\times10^{-11}$	1.8±0.5
Carr and Swenson[f]			$(24.3\pm1.5)\times10^{-10}$	$(9.0\pm0.3)\times10^{-11}$	1.34±0.08
This work	$(-2.7\pm0.06)\times10^{-3}$	$(-4.0\pm0.2)\times10^{-3}$			6.65±3

[a] Thermal expansion data are analyzed on the basis of the following equations: $\beta=+1/V(\partial V/\partial T)_P=\beta_{en}+\beta_{gn}$, where $\beta_{en}=(k_n\gamma T/V)\times(d\ln\gamma/d\ln V)$. Values of $d\ln\gamma/d\ln V$ were calculated from thermal expansion data using $\gamma=1.35$ mJ/mole °K, $k_n=1.34\times10^{-6}$ atm^{-1} [Brandt and Ginzburg (Ref. 17)], and $V=9.87$ cm^3/mole. See B. F. Figgins, G. O. Jones, and D. P. Riley, Phil. Mag. **1**, 747 (1956).

[b] J. L. Olsen, Helv. Phys. Acta **32**, 310 (1959).

[c] See Ref. 30.

[d] G. K. White, in *Proceedings of the Eighth International Conference on Low-Temperature Physics, London, 1962*, edited by R. O. Davies (Butterworths Scientific Publications, Ltd., London, 1963), p. 394.

[e] K. Andres, Phys. Kondensierten Materie **2**, 294 (1964).

[f] R. H. Carr and C. A. Swenson, Cryogenics **4**, 76 (1964).

sets of data are displayed in Fig. 10. Caplan and Chanin attribute the large scatter in their low-temperature data to difficulties in their temperature measurements using He^3 vapor pressure thermometry. They also point out that there is some question about whether their method yields reliable thermodynamic equilibrium values. The method of Caplan and Chanin is based on detection of the position of a superconducting phase boundary in a long cylindrical specimen. The specimen is held in a magnetic field with a controlled longitudinal gradient. As remarked by these authors, any effect which impedes the free motion of the phase boundary will produce deviations from equilibrium values of H_c. Whether for these or for other reasons, it seems likely from Fig. 10 that Caplan and Chanin's data are not reliable below about 0.6°K.

It is also of interest to compare experimental results for the energy gap at 0°K in aluminum with values calculated from our results using the BCS theory. The basic theoretical equation is

$$\frac{VH_0^2}{2\pi\gamma T_c^2}=\frac{3}{4\pi^2}\left(\frac{2\Delta(0)}{kT_c}\right)^2, \tag{22}$$

and the "simple" BCS prediction is

$$2\Delta(0)/kT_c=3.528. \tag{23}$$

The BCS relation assumes that the electron-phonon interaction responsible for superconductivity is isotropic in momentum space. Clem[25] has calculated the effects of anisotropy in the superconducting energy gap on the thermodynamic properties of superconductors. His calculation leads to the following modifications in (22) and (23).

$$VH_0^2/2\pi\gamma T_c^2=(3/4\pi^2)[2\Delta(0)/kT_c]^2(1+\langle a^2\rangle), \tag{24}$$

$$2\Delta(0)/kT_c=3.528(1-\tfrac{3}{2}\langle a^2\rangle), \tag{25}$$

where $\langle a^2\rangle$, the mean squared anisotropy, is the average over the Fermi surface of the square of the deviation of the energy-gap parameter from its average value.

Experimental evidence with respect to gap anisotropy in aluminum is reasonably consistent [although the average value of $\Delta(0)$ seems much less so]. Masuda and Redfield[26] found that their nuclear spin relaxation measurements in aluminum were consistent with an energy gap of $3.2kT_c$ smeared by about 10%. The data of Biondi, Garfunkel, and Thompson[27] may be interpreted to show two distinct gaps in aluminum, at about $3.05kT_c$ and $3.50kT_c$. This is presumably due to anisotropy. Markowitz and Kadanoff[28] estimate that $\langle a^2\rangle=0.011$ for aluminum, by analysis of measurements of the critical temperature versus impurity doping by Chanin *et al.*[29] All of these results suggest $\langle a^2\rangle\cong0.01$ as the best estimate of the anisotropy for use in Clem's formulas.

Comparison between the present experimental results and BCS theoretical values with and without the anisotropy correction are given in Table V. Clem's expressions have also been used to compute $D(t)$. As shown by the solid curve in Fig. 10, there is very good agreement with the experimental data if one assumes $\langle a^2\rangle=0.013\pm0.002$.

For further comparison other experimental values of the energy gap in aluminum are collected in Table VI. The results are grouped to differentiate measurements on bulk specimens from observations on thin films. The various bulk measurements in Table VI show fair internal consistency and (considering the analysis and interpretation involved) are not in strong disagreement with our derived values. The thin-film data show poor internal consistency although averaging to a value near those shown in Table V.

[25] J. R. Clem, Phys. Rev. **153**, 449 (1967); Ann. Phys. (N.Y.) **40**, 268 (1966).

[26] Y. Masuda and A. Redfield, Phys. Rev. **125**, 159 (1962).

[27] M. A. Biondi, M. P. Garfunkel, and W. A. Thompson, Phys. Rev. **136**, A1471 (1964).

[28] D. Markowitz and L. P. Kadanoff, Phys. Rev. **131**, 563 (1963).

[29] G. Chanin, E. A. Lynton, and B. Serin, Phys. Rev. **114**, 719 (1959).

Previous work on the weak-coupling superconductors, Sn and In, showed much better agreement between thermodynamically derived values of $\Delta(0)$ and direct measurements via tunneling or electromagnetic absorption.[1] Since aluminum, by all evidence, is more weakly coupled than either Sn or In, even closer agreement might have been expected in this case. This expectation is evidently not fulfilled and the substantial variation among the values in Table VI suggests that some surface peculiarity of aluminum may be responsible.

Our pressure effect results are listed with data from comparable investigations in Table VII. The most closely related work is that of Gross and Olsen[30] for which the derived values of (dH_0/dP) and $(\partial H_c/\partial P)_{T=T_c}$ differ, respectively, by $+15\%$ and $+20\%$ from our values. Part of this difference is due to the method of analysis since Gross and Olsen assume the similarity principle to apply and also disregard the deviation of $H_c(T)$ from the parabolic law. On the basis of the present measurements of $D(t)$, the analysis of Gross and Olsen would be expected to yield values of (dH_0/dP) and $(\partial H_c/\partial P)_{T=T_c}$ about 5% too large. Thus the remainder of the discrepancy is unexplained.

Gross and Olsen give a value of $d\ln\gamma/d\ln V$ of about 8.5, depending on the slope chosen to represent $H_c(T)$ near T_c. The value for $d\ln\gamma/d\ln V$ listed for their data in Table VII is computed from (11) using their values of (dH_0/dP) and $(\partial H_c/\partial P)_{T=T_c}$ and our values for H_0, T_c, k_n, and $(\partial H_c/\partial T)_P$ (at T_c). Considering experimental uncertainties and differences in the mode of analysis, agreement is reasonably good.

Both our value of $d\ln\gamma/d\ln V$ and that calculated from Gross and Olsen's work disagree with the values calculated from thermal expansion data listed in Table VII. The thermal expansion measurements give $d\ln\gamma/d\ln V$ directly, while in the absence of precise critical-field data below $t=0.25$, $d\ln\gamma/d\ln V$ must be inferred from similarity analysis of the critical-field data using Eq. (11). The two terms in brackets in (11) are of nearly the same magnitude and opposite sign, hence the resulting value of $d\ln\gamma/d\ln V$ is quite susceptible to error. A better determination of $d\ln\gamma/d\ln V$ for Al from critical-field data must await the extension of precise measurements to higher pressures and much lower temperatures where the data can be analyzed to give $d\ln\gamma/d\ln F$ directly.

Inconsistency between thermal expansion and critical-field determinations of $d\ln\gamma/d\ln V$ has also been observed in other materials. In the case of Pb and Ta, the value of $d\ln\gamma/d\ln V$ determined from low temperature $H_c(P, T)$ data[31] (without recourse to the similarity principle) is roughly a factor of 3 larger than the value obtained from thermal expansion measurements.[32] This is about the same degree of inconsistency as we report here for aluminum. At present, we know of no explanation for this inconsistency. We are now extending $H_c(P, T)$ measurements on Pb to 0.3°K in order to obtain a more precise determination of $d\ln\gamma/d\ln V$.

All values of $d\ln\gamma/d\ln V$ for Al listed in Table VII, including our result, are considerably larger than the nearly free-electron model result of 2/3. Other authors[30,33] have pointed out that this effect may be due to pressure sensitivity of parts of the Fermi surface near zone boundaries, since aluminum, with three electrons per atom, has a Fermi surface very close to zone boundaries.[33–35] Evidence that this idea is qualitatively correct comes from recent de Haas–van Alphen effect measurements of the effect of pressure on the Fermi surface of aluminum by Melz.[36] Melz found changes in parts of the Fermi surface which disagree with the predictions of the nearly free-electron model by over an order of magnitude.

[30] D. Gross and J. L. Olsen, Cryogenics **1**, 91 (1960).

[31] For Pb see Ref. 2; for Ta see C. H. Hinrichs and C. A. Swenson, Phys. Rev. **123**, 1106 (1961).

[32] For a review see J. G. Collins and G. K. White, in *Progress in Low-Temperature Physics*, edited by C. J. Gorter (North-Holland Publishing Co., Amsterdam, 1964), Vol. IV, p. 450.

[33] P. G. Klemens, Phys. Rev. **120**, 843 (1960).

[34] W. A. Harrison, in *Physics of Solids at High Pressures*, edited by C. Tomizuka and R. Emrick (Academic Press Inc., New York, 1965).

[35] W. A. Harrison, *Pseudopotentials in the Theory of Metals* (W. A. Benjamin, Inc., New York, 1966), Chap. 3.

[36] P. J. Melz, Phys. Rev. **152**, 540 (1966).